the value of 840 ± 50 $cm^{-1}$ found from the temperature dependence of magnetic susceptibility measurements.[4,5]

From Figure 3, three transitions from the $^3E''(A_1' + A_2')$ spin–orbit level to the $^3A_2''(A_1'' + E')$ ground-state spin–orbit levels are electric dipole allowed, corresponding to $A_1' \rightarrow E'(\sigma)$, $A_2' \rightarrow E'(\sigma)$, and $A_2' \rightarrow A_1''(\pi)$. The two $\sigma$ polarized transitions will occur close together, as the $A_1'$ and $A_2'$ spin–orbit states belonging to the $^3E''$ multiplet are only separated by ≈5 $cm^{-1}$. The emission origins at 6859 and 6809 $cm^{-1}$ are therefore attributed to $^3E''(A_1' + A_2') \rightarrow {}^3A_2''(E')$ and $^3E''(A_2') \rightarrow {}^3A_2''(A_1'')$, but without polarization data it is difficult to discriminate further. However, the vibrational bands associated with the weaker progression based on the 6859-$cm^{-1}$ origin are distinctively broader and asymmetric, indicative of the $^3E''(A_1' + A_2') \rightarrow {}^3A_2''(E')$ transition due to the zero-field splitting of the $A_1'$ and $A_2'$ spinor levels.

From the above assignments, the zero-field splitting of the $^3A_2''(A_1'' + E')$ ground state is quite large, ≈50 $cm^{-1}$, with the E' level at lower energy. Although at this stage it is not possible to undertake a full $d^3d^3$ pair calculation which includes the spin–orbit interaction, due to the large basis size of 14 400, some measure of the zero-field splitting of the $^3A_2''(^3A_2{}^3A_2)$ pair state can be gained from the following perturbation treatment.

In the Mo–Mo $\sigma$ bond limit, the $^3A_2''$ pair state derives from the $t_{2e}^2$ single-ion $^3A_2$ state for which the zero-field splitting is described by the spin-Hamiltonian

$$\mathcal{H}_{eff} = D[S_z^2 - S(S+1)/3]$$

with eigenvalues $|M = 0\rangle = -2D/3$ and $|M = \pm 1\rangle = D/3$. Second-order spin–orbit coupling must be invoked in order to split the $|M = 0\rangle$ and $|M = \pm 1\rangle$ spin levels of the $^3A_2$ state. Of the $t_{2e}^2$ excited states $^1E$ and $^1A_1$, only the $^1A_1$ level is coupled to the $^3A_2$ ground state according to

$$\langle {}^3A_2\ M = 0|\zeta \sum_i l_z s_z|{}^1A_1\rangle = i\zeta$$

where $\zeta$ is the one-electron spin–orbit coupling constant. For second-order perturbation, the energy shift of the $|M = 0\rangle$ level is given by

$$\langle {}^3A_2|\mathcal{H}_{so}|{}^1A_1\rangle\langle {}^1A_1|\mathcal{H}_{so}|{}^3A_2\rangle / E({}^3A_2 - {}^1A_1)$$

resulting in the zero-field splitting

$$D = E(|M = \pm 1\rangle - |M = 0\rangle) = \zeta^2/\Delta E$$

where $\Delta E = 12B + 4C$ is the energy difference between the $^1A_1$ and $^3A_2$ states and $B$ and $C$ are the usual Racah electron repulsion parameters.[3] For the single-ion $^3A_2$ state the $|M = 0\rangle$ level is predicted to lie at lower energy, whereas for the $^3A_2''(^3A_2{}^3A_2)$ pair state it can be shown that the splitting is reversed with the $|M = \pm 1\rangle$ level at lower energy. For Mo(III), the free ion spin–orbit coupling constant $\zeta$ is approximately 800 $cm^{-1}$, while from the low-temperature absorption spectrum of $Cs_3Mo_2Cl_9$, the separation of the single-ion $^1A_1$ and $^3A_2$ states is about 11 000 $cm^{-1}$. From these values, a zero-field splitting of $D \approx 60$ $cm^{-1}$ is calculated for the $^3A_2''$ pair state with the $E'(M \pm 1)$ spin–orbit level at lower energy, in agreement with the above analysis. Allowing for an appropriate reduction in $\zeta$ from the free ion value ($\zeta \approx 600$ $cm^{-1}$ was found from a spectroscopic study[9] of $MoCl_6^{3-}$), the observed zero-field splitting of ≈50 $cm^{-1}$ seems quite reasonable.

**Registry No.** $Cs_3Mo_2Cl_9$, 29013-02-3; Mo, 7439-98-7.

---

Contribution from the Institut de Chimie Minérale et Analytique, Université de Lausanne, Place du Château 3, Lausanne CH-1005, Switzerland, and Department of Chemistry, University of the Orange Free State, Bloemfontein 9300, South Africa

# $^{13}C$ and $^{17}O$ NMR Studies of the Solution and Equilibrium Behavior of Selected Oxocyanorhenate(V) Complexes

Andreas Roodt,*[,1] Johann G. Leipoldt,[1] Lothar Helm,[2] and André E. Merbach*[,2]

*Received January 23, 1992*

Carbon-13 and oxygen-17 NMR spectroscopies were utilized to study the solution and protonation equilibrium behavior of the *trans*-dioxotetracyanorhenate(V) ion. The $pK_{a_1}$ and $pK_{a_2}$ values for the successive dissociation of the $[ReO(H_2O)(CN)_4]^-$ complex were determined from $^{13}C$ and $^{17}O$ NMR chemical shifts as 1.31 (7) and 3.72 (5), respectively. The dimeric species $[Re_2O_3(CN)_8]^{4-}$ (formed by condensation of $[ReO(OH)(CN)_4]^{2-}$ ions) and the monosubstituted product $[ReO(NCS)(CN)_4]^{2-}$ were also studied, and results were correlated with NMR measurements in DMSO solutions. The $^{17}O$ chemical shifts for the different species studied showed a direct relationship with X-ray crystal structure and infrared data and with the electron density on the coordinated oxygen ligands and demonstrated the effectiveness of $^{17}O$ NMR spectroscopy for characterization of these types of complexes.

## Introduction

There have been differences in opinion in the literature on the nature of the different Re(V) species formed in solution when the *trans*-$[ReO_2(CN)_4]^{3-}$ complex is dissolved in acidic solution.[3,4] We have however eliminated the uncertainties by several X-ray crystal structure determinations[5] and kinetic[6] and infrared[7] studies over the last few years and showed that the aqueous acid chemistry of the $[ReO_2(CN)_4]^{3-}$ complex may be described by the reactions in Scheme I. Similar behavior has been confirmed previously for the isoelectronic Mo(IV)[8] and W(IV)[9] systems and recently

**Scheme I**

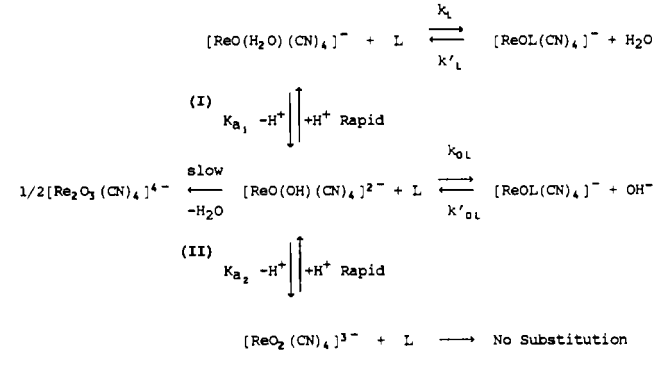


(1) University of the Orange Free State.
(2) Université de Lausanne.
(3) Chakravorti, M. C. *J. Inorg. Nucl. Chem.* **1972**, *34*, 893.
(4) Toppen, D.; Murmann, R. K. *Inorg. Chem.* **1973**, *12*, 1611.
(5) (a) Purcell, W.; Roodt, A.; Basson, S. S.; Leipoldt, J. G. *Transition Met. Chem. (London)* **1989**, *14*, 369. (b) Basson, S. S.; Leipoldt, J. G.; Roodt, A.; Purcell, W. *Transition Met. Chem. (London)* **1987**, *12*, 82. (c) Purcell, W.; Roodt, A.; Basson, S. S.; Leipoldt, J. G. *Transition Met. Chem. (London)* **1989**, *14*, 5. (d) Purcell, W.; Roodt, A.; Basson, S. S.; Leipoldt, J. G. *Transition Met. Chem. (London)* **1990**, *15*, 239.
(6) (a) Purcell, W.; Roodt, A.; Basson, S. S.; Leipoldt, J. G. *Transition Met. Chem. (London)* **1989**, *14*, 224. (b) Purcell, W.; Roodt, A.; Leipoldt, J. G. *Transition Met. Chem. (London)* **1991**, *17*, 339.
(7) Leipoldt, J. G.; Basson, S. S.; Roodt, A.; Purcell, W. *Transition Met. Chem. (London)* **1987**, *12*, 209.

0020-1669/92/1331-2864$03.00/0 © 1992 American Chemical Society

also for the dioxotetracyanotechnetate(V)[10] complex, the latter serving as a model for certain Tc(V) radiopharmaceuticals.[10]

Since the usefulness of oxygen-17 NMR spectroscopy as a structural and kinetic probe has been demonstrated previously in different systems,[11] for example in the complex oligomeric Mo(IV) aqueous[12] system, we have undertaken this investigation to further study the solution chemistry of the dioxotetracyanorhenate(V) system and to compare the results obtained from NMR measurements with those gathered by solid-state and complex formation kinetic studies. This investigation also forms a part of a complete NMR study on the solvent exchange of these and similar complexes serving as model systems for certain radiopharmaceuticals.[10] The careful characterization of different species by NMR spectroscopy in such a study was therefore of prime importance, the results obtained for the Re(V) system being described in this paper.

## Experimental Section

**General Considerations.** $K_3ReO_2(CN)_4$ was prepared as was described previously.[7] Unless otherwise noted, all chemicals were of reagent grade and all experiments were performed aerobically in aqueous media. All measurements were performed on solutions with a total rhenium concentration of 0.2 *m* at an ionic strength of 1 *m* ($KNO_3$ supporting electrolyte) unless otherwise stated. A calomel electrode from Radiometer (GK2322C) and a Metrohm Herisau E603 pH meter were used for pH measurements. Standard buffer solutions and standardized 0.100 M $HNO_3$ and NaOH solutions were used for calibration. In the pH dependence studies, microtitrations of a 2-mL solution of the metal complex with standardized 10 M NaOH, 15 M $HNO_3$, and 9 M HCl solutions with a micropipette were performed inside the NMR tube.

**NMR Measurements.** All NMR experiments were done on a Bruker AM-400 spectrometer (9.4-T cryomagnet) at 54.227 MHz (oxygen-17) and 100.6 MHz (carbon-13). The external standard used in the $^{13}C$ studies was 3-(trimethylsilyl)tetradeuteriopropionate (3TMSP), while in the $^{17}O$ studies the shift was referenced to the free water peak and measured with respect to the nitrate ion, $\delta(NO_3)$ = 413 ppm, as internal reference. When necessary, the free water peak was also used as a quantitative reference. All aqueous solutions used for oxygen-17 measurements contained 5% oxygen-enriched water. Complexes containing equilibrated oxygen-17 are asterisked, e.g. [*O=Re—*$OH_2$], for simplicity throughout. The temperature was controlled by a Bruker B-VT 1000 unit and was measured by substituting the sample tube for one containing a Pt(100) resistor.[13] In the $^{13}C$ study the following NMR parameters were used: Over a frequency range of 22.7 kHz 16K data points were acquired at a pulse length of 20 μs. An exponential line broadening of 12 Hz was used with 1.4-s time intervals between transients, of which between 1000 and 3000 were added prior to Fourier transformation. Unless otherwise stated in the figure captions, the parameters for the general collection of $^{17}O$ NMR spectra were the following: A frequency range of 55.5 kHz was used to collect 2K data points with a pulse length of 15 μs and exponential line broadening of 80–100 Hz. The time between transients, of which between 1000 and 30 000 were added prior to Fourier transformation, was 18 ms.

**Preparation of $^{17}O$-Enriched Complexes.** The basic preparations of all these complexes have been described previously;[7] however, modifications had to be introduced to ensure maximum oxygen-17 enrichment with minimal use of oxygen-17-enriched water.

**Tetramethylammonium Aquaoxotetracyanorhenate(V) Tetrahydrate, $(Me_4N)[Re^*O(H_2{}^*O)(CN)_4]\cdot 4H_2{}^*O$.** To a cooled solution of 150 mg (0.34 mmol) of $K_3ReO_2(CN)_4$ in 400 μL of 10% $H_2{}^{17}O$ was added 50 μL (0.75 mmol) of $HNO_3$(conc), and the mixture was allowed to stand for 10 min to ensure complete exchange. A solution of 160 mg (1.46 mmol) of $Me_4NCl$ in 400 μL of normal water was slowly added, and the light purple crystalline material was decanted, filtered off, and dried in a fume hood (140 mg, yield 90%). NMR solution: 37 mg/1.6 mL of DMSO (0.05 m*m*).

**Tetraphenylphosphonium Tetracyanohydroxooxorhenate(V) Hydrate, $(PPh_4)_2[Re^*O(^*OH)(CN)_4]\cdot H_2{}^*O$.** To a cooled solution of 150 mg (0.34 mmol) of $K_3ReO_2(CN)_4$ in 400 μL of 10% $H_2{}^{17}O$ was added 50 μL (0.75 mmol) of $HNO_3$(conc), and the mixture was allowed to stand for 10 min to ensure complete exchange. Then 50 μL (0.50 mmol) of a 10 *m* KOH solution was added, followed by the slow addition of a solution of 260 mg (0.69 mmol) of $PPh_4Cl$ in 400 μL of normal $H_2O$. The light brown crystalline product was filtered off and dried in a fume hood (330 mg, yield 90%). NMR solution: 80 mg/1.6 mL of DMSO (0.046 m*m*).

**4,4′-Bipyridinium Tetracyanooxothiocyanatorhenate(V), $(4,4'\text{-}bpyH_2)[Re^*O(NCS)(CN)_4]$.** To a cooled solution of 100 mg (0.23 mmol) of $K_3ReO_2(CN)_4$ in 400 μL of 10% $H_2{}^{17}O$ was added 35 μL (0.52 mmol) of $HNO_3$(conc), and the solution was allowed to stand for 10 min to ensure complete exchange. To this solution was added 100 mg (1 mmol) of KNCS, and the mixture was again allowed to stand for 10 min to ensure complete substitution, after which a solution containing 50 mg (0.32 mmol) of 4,4′-bipyridine and 40 μL (0.60 mmol) of $HNO_3$(conc) in 400 μL of normal water was slowly added. The resulting purple-brown crystalline solid was filtered off and dried in a fume hood (100 mg, yield 90%). NMR solution: 45 mg/1.6 mL of DMSO (0.055 m*m*).

## Results

**Equilibrium Studies.** A carbon-13 NMR study was first undertaken in order to investigate the species behavior in solution, since $^{13}C$ spectra were expected to be much simpler than those of $^{17}O$. Because the two protonation steps of the $[ReO_2(CN)_4]^{3-}$ complex (equilibria I and II in Scheme I) occur in acidic medium (see Table I), the pH dependence of the spectra was studied in the pH range 0–8. Only one signal, resulting from the fast proton exchange between the dioxo, oxo hydroxo, and oxo aqua species (Scheme I), was observed. The pH dependence of the chemical shift, δ, related to the population average of the different species, is illustrated in Figure 1, and the relationship at any $[H^+]$ is given by eq 1, where $\delta_a$, $\delta_h$, and $\delta_o$ represent the $^{13}C$ chemical shifts

$$\delta = \frac{\delta_a[H^+]^2 + K_{a_1}\delta_h[H^+] + K_{a_1}K_{a_2}\delta_o}{[H^+]^2 + K_{a_1}[H^+] + K_{a_1}K_{a_2}} \quad (1)$$

resulting from the aqua oxo, hydroxo oxo, and dioxo species, respectively, and $K_{a_1}$ and $K_{a_2}$ are the acid dissociation constants of the $[ReO(H_2O)(CN)_4]^-$ ion. A least-squares fit of the δ vs $[H^+]$

**Table I.** Summary of Equilibrium Data for $[ReO(H_2O)(CN)_4]^-$ at 25.0 °C and μ = 1.0–1.4 *m* ($KNO_3$)

| method | $pK_{a_1}$ | $pK_{a_2}$ | ref |
|---|---|---|---|
| potentiometric | 1.4 | 4.2 | 3 |
| potentiometric | | 3.71 | 4 |
| kinetic | 1.35 (8) | | 6 |
| $^{13}C$ NMR[a] | 1.31 (7) | 3.72 (5) | this work |
| $^{17}O$ NMR[b] | | 3.66 (5) | this work |

[a] Equation 1 (data in Figure 1), where $\delta_a$ = 128.0 (2), $\delta_h$ = 134.5 (2), and $\delta_o$ = 141.6 (1) ppm. [b] Equation 2 (data in Figure 5, at 15.0 °C), where $\delta(ORe\mathit{O})$ = 463 (1) and $\delta(\mathit{O}ReOH)$ = 443 (1) ppm.

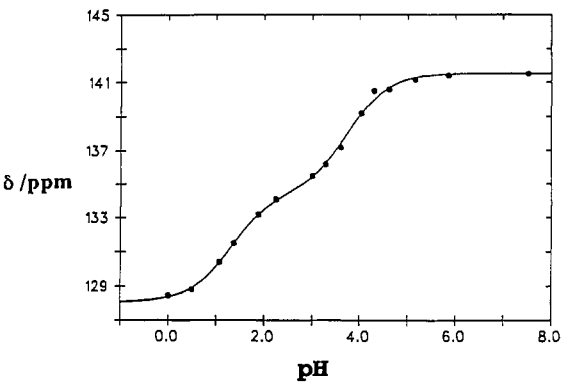


**Figure 1.** Influence of pH on the $^{13}C$ chemical shift, δ, for the Re(V) system at 25.0 °C ([Re] = 0.2 *m*, μ = 1–1.4 *m* ($KNO_3$), NMR reference = 3TMSP).


(8) (a) Potgieter, I. M.; Basson, S. S.; Roodt, A.; Leipoldt, J. G. *Transition Met. Chem. (London)* **1988**, *13*, 209 and references within. (b) Robinson, P. R.; Schlemper, E. O.; Murmann, R. K. *Inorg. Chem.* **1975**, *14*, 2035.

(9) (a) Roodt, A.; Leipoldt, J. G.; Basson, S. S.; Potgieter, I. M. *Transition Met. Chem. (London)* **1988**, *13*, 336. (b) Roodt, A.; Leipoldt, J. G.; Basson, S. S.; Potgieter, I. M. *Transition Met. Chem. (London)* **1990**, *15*, 439 and references within.

(10) Roodt, A.; Leipoldt, J. G.; Deutsch, E. A.; Sullivan, J. C. *Inorg. Chem.* **1992**, *31*, 1080.

(11) Klemperer, W. G. *Angew. Chem., Int. Ed. Engl.* **1978**, *17*, 246.

(12) Richens, D.; Helm, L.; Pittet, P.-A.; Merbach, A. E. *Inorg. Chim. Acta* **1987**, *132*, 85.

(13) Ammann, C.; Meier, P.; Merbach, A. E. *J. Magn. Reson.* **1982**, *46*, 319.

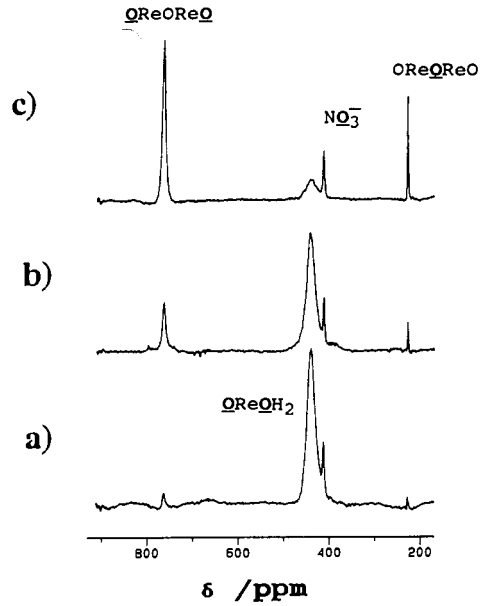


**Figure 2.** Time dependence of a Re(V) solution at pH = 1.30, monitored by $^{17}O$ NMR spectroscopy at 25.0 °C ([Re] = 0.2 *m*, $\mu$ = 1.0 *m* ($KNO_3$), NMR reference = $H_2{}^{17}O$) after (a) 3 min, (b) 1 h, and (c) 6 h. For NMR parameters, see Experimental Section; for signal identification, see Table II.

data yielded values for all the parameters, which are reported in Table I.

**Oxygen Exchange.** Figure 2 illustrates the $^{17}O$ spectra that were observed at pH ~1.30, where $[ReO(H_2O)(CN)_4]^-$ is the main Re(V) species in solution. The first spectrum, Figure 2a, was recorded after 3 min, and a substantial signal at about 440 ppm, and *not* around 0 ppm as might be expected for coordinated water,[14] was observed. Integration of this signal revealed a Re:O ratio of 1:2, originating from a fast exchange between the aqua and oxo sites in the aqua oxo complex. This signal showed a slow decrease with time, accompanied by the simultaneous formation of two signals at ca. 760 and 220 ppm, respectively (Figure 2b,c). The rate of formation of these two signals corresponded to the expected slow formation rate of the dimeric species, $[Re_2O_3(CN)_8]^{4-}$. It was found that the $\mu$-O exhibited a very slow relaxation rate, and upon quantitative recording of spectra, with appropriate repetition time (see Figure 3), the peaks at $\delta$ = 765 and 229 ppm could be assigned to the terminal and $\mu$-oxo sites in the $[Re_2O_3(CN)_8]^{4-}$ ion, respectively, specifically since an oxygen molar ratio of 2:1 for the two signals was obtained, consistent with that expected for the linear O═Re—O—Re═O entity in the dimeric species.

Spectra a and c of Figure 4 show the effect observed upon addition of alkali (final pH = 8) to the solution described in Figure 2c, taking into account that the $pK_{a_2}$ for this system is 3.72. A shift in this signal to $\delta$ = 463 ppm was observed, accompanied by a considerable sharpening of the signal (Figure 4c, $\delta$(*O*ReO)). The integral of this shifted signal was the same as that found for the signal at approximately 440 ppm (consistent with a 2:1 molar ratio for O:Re), indicating the formation of the $[Re(*O)_2(CN)_4]^{3-}$ species.

Figure 4 further illustrates the effect of excess monodentate ligand (e.g. thiocyanate) on the $[*ORe(H_2{}^*O)(CN)_4]^-$ complex. Upon addition of solid KNCS to a solution (pH = 1.10) showing the signal at ca. 440 ppm, the disappearance of this signal was observed, corresponding to the simultaneous formation of a signal at ca. 884 ppm ($\delta$(*O*ReNCS)). In Figure 4b, both the signals of the dimeric species and the formation of the signal of the $[Re^*O(NCS)(CN)_4]^{2-}$ ion can be clearly seen, and furthermore, the formation of the thiocyanato complex can be monitored with ease in the presence of the $[Re_2O_3(CN)_8]^{4-}$ complex. The rate

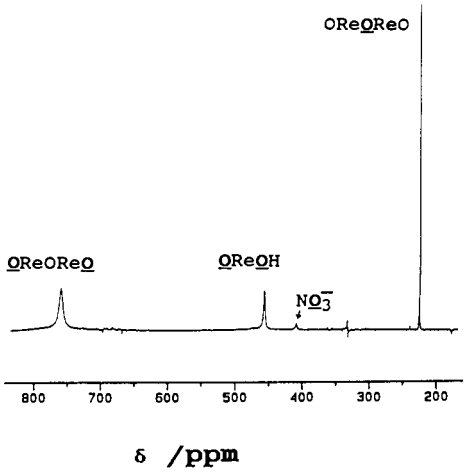


**Figure 3.** Quantitative oxygen-17 NMR spectrum showing the $^{17}O$ signals of the dimeric species $[Re_2O_3(CN)_8]^{4-}$ ($T$ = 25.0 °C, [Re] = 0.2 *m*, $\mu$ = 1.0 *m* ($KNO_3$), NMR reference = $H_2{}^{17}O$). NMR parameters: frequency range = 55.5 kHz, number of data points collected = 32K, pulse width = 15 $\mu$s, number of transients added = 2800, time between transients = 0.8 s, exponential line broadening = 3 Hz.

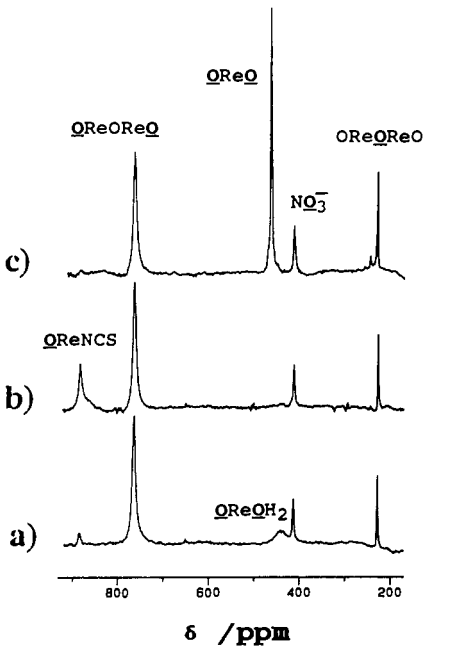


**Figure 4.** Qualitative $^{17}O$ NMR spectra of a Re(V) solution at (a) pH = 1.10, showing the effect of added (b) $NCS^-$ and (c) $OH^-$ (pH = 8) at 25.0 °C (NMR standard = $H_2{}^{17}O$, [Re] = 0.2 *m*, $\mu$ = 1–1.4 *m* ($KNO_3$)). For NMR parameters, see Experimental Section; for signal identification, see Table II.

increase of this signal corresponded to the previously observed formation rate of the $[ReO(NCS)(CN)_4]^{2-}$ complex.[6] The integral of the newly formed signal at 884 ppm was only half that of the signal at approximately 440 ppm, which is consistent with an expected Re:O molar ratio of 1:1 in the $[Re^*O(NCS)(CN)_4]^{2-}$ ion. Upon addition of alkali to this solution containing the thiocyanato complex ($pH_{fin}$ = 8), the 884 ppm signal disappeared rapidly (hydrolysis of the coordinated $NCS^-$ ligand), forming a signal at 463 ppm ($\delta$(*O*ReO)) (Figure 4c) with a Re:O ratio again 2:1, similar to the case described above for the dioxo species. This substitution/hydrolysis process is reversible by simple pH manipulation.

The effect of pH on the $^{17}O$ spectra in the range 0–8 was studied and is illustrated in Figure 5. Only one signal was observed over the entire pH range investigated, with only a significant change in chemical shift around the $pK_{a_2}$ value of the $[ReO(H_2O)(CN)_4]^-$ ion. It was clear that, in the case of the $[Re^*O(^*OH)(CN)_4]^{2-}$ complex, as was found for the aqua species, also only the weighted

(14) Richens, D. R.; Helm, L.; Pittet, P.-A.; Merbach, A.; Nicolo, F.; Chapuis, G. *Inorg. Chem.* **1989**, *28*, 1394.

**Table II.** Comparison of Structural, Infrared, and $^{17}O$ NMR Data for the Dioxotetracyanorhenate(V) System

| complex | site | bond length (Å) | $\nu$(Re—O)[a] ($cm^{-1}$) | $^{17}O$ chem shift (ppm) ID[b] | DMSO | $H_2O$[c] |
|---|---|---|---|---|---|---|
| $[ReO(H_2O)(CN)_4]^-$ | Re=O | 1.667(8)[d] | 1038 | $\delta(OReOH_2)$ | 874 | |
| $[ReO(NCS)(CN)_4]^{2-}$ | Re=O | 1.67(1)[e] | 1010 | $\delta(OReNCS)$ | 869 | 884 |
| $[Re_2O_3(CN)_8]^{4-}$ | Re=O | 1.69(1)[f] | 995 | $\delta(OReORe O)$ | | 765 |
| $[ReO(OH)(CN)_4]^{2-}$ | Re=O | 1.70(1)[g] | 952 | $\delta(OReOH)$ | 752 | |
| $[ReO_2(CN)_4]^{3-}$ | Re=O | 1.783(1)[h] | 785 | $\delta(OReO)$ | | 463 |
| $[Re_2O_3(CN)_8]^{4-}$ | Re—$\mu$-O | 1.921(1)[f] | 700 | $\delta(OReOReO)$ | | 229 |
| $[ReO(OH)(CN)_4]^{2-}$ | Re—OH | 1.90(1)[g] | 660 | $\delta(OReOH)$ | 119 | |
| $[ReO(H_2O)(CN)_4]^-$ | Re—$OH_2$ | 2.142(7)[d] | 600 | $\delta(OReOH_2)$ | −19 | |

[a] Reference 7. [b] Signal identification in Figures 2–4 and 6. [c] 25 °C, $\mu$ ca. 1 *m* ($KNO_3$). [d] Reference 5d. [e] Reference 5a. [f] Reference 5b. [g] Reference 5c. [h] Reference 17.

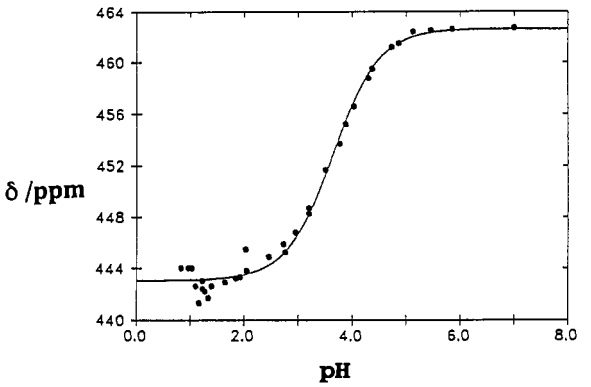


**Figure 5.** Influence of pH on the $^{17}O$ chemical shift, $\delta$, for the Re(V) system at 15.0 °C ([Re] = 0.2 *m*, $\mu$ = 1–1.4 *m* ($KNO_3$), NMR reference = $H_2{}^{17}O$).

*average* oxygen-17 signal of the oxo and the hydroxo sites is observed. A significant broadening of the signal was also observed, resulting in poor chemical shift data at pH < 2. The oxygen-17 data as shown in Figure 5 were fitted to eq 2, wherein $\delta(OReO)$

$$\delta = \frac{\delta(OReOH)\,[H^+] + \delta(OReO)\,K_{a_2}}{[H^+] + K_{a_2}} \qquad (2)$$

represents the chemical shift of the dioxo signal and $\delta(OReOH)$ the chemical shift of the average signal of the oxo/hydroxo moiety. The results are reported in Tables I and II.

In order to separately observe the $^{17}O$ signals of the four oxygen sites in the $[Re^*O(^*OH)(CN)_4]^{2-}$ and $[Re^*O(H_2{}^*O)(CN)_4]^-$ ions, the signal behavior was investigated in a solvent that will limit both water and proton exchange. Figure 6 illustrates the spectra obtained in dimethyl sulfoxide, which was the only solvent that allowed sufficient solubility of the different complexes for acceptable NMR spectra, in spite of the fact that organic cations were used in an attempt to increase the solubility of the different species in organic media (Experimental Section). Care was taken to record the spectra as soon as the solid samples were dissolved in the DMSO solution in order to limit any DMSO/water exchange as far as possible. In the case of the aqua complex, a slow shift in the oxo signal was observed upon standing in the DMSO solution (the coordinated aqua ligand probably being replaced by a DMSO molecule), but it was assumed that the chemical shift determined from the first spectrum after dissolution of the solid was close to the true chemical shift for the Re=O signal of the $[ReO(H_2O)(CN)_4]^-$ ion. In the case of the hydroxo complex, no change in chemical shift with time could be detected; only a total decomposition was observed after ca. 1 h. The spectrum of the $[Re^*O(NCS)(CN)_4]^{2-}$ complex is included (Figure 6c) for correlation between the aqueous and DMSO data. The chemical shift data for all these complexes are summarized in Table II.

## Discussion

In the case of the $^{13}C$ study, only one signal, without indication of line broadening, was observed over the entire pH range investigated, and it was therefore clear that the proton exchange is rapid relative to the NMR time scale, as may be anticipated.

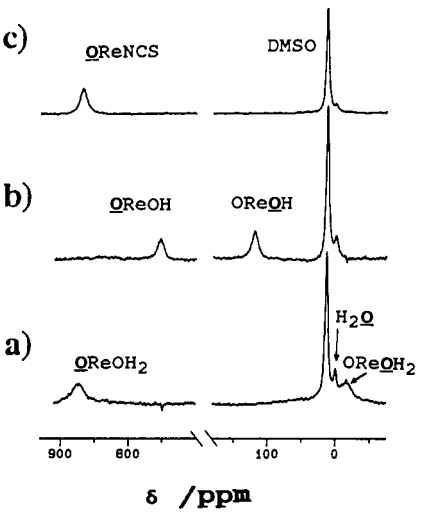


**Figure 6.** Oxygen-17 NMR spectra of $^{17}O$-enriched oxo cyano complexes in DMSO at 25 °C: (a) $[Re^*O(H_2{}^*O)(CN)_4]^-$; (b) $[Re^*O(^*OH)(CN)_4]^{2-}$; (c) $[Re^*O(NCS)(CN)_4]^{2-}$. For solution preparation, see Experimental Section; for signal identification, see Table II.

Of significance is the fact that $^{13}C$ NMR spectroscopy provides an excellent means for the accurate determination of the acid dissociation constants (Table I), not always possible as a result of, for example in the present case, the formation of the dimeric species (Scheme I), having a large molar absorptivity which can easily influence UV/visible absorption measurements in spectrophotometric studies. The formation of the $[Re_2O_3(CN)_8]^{4-}$ ion was easily observed in this study, showing also, as to be expected, only one signal, since all eight of the carbon atoms of the cyano ligands are equivalent. The chemical shift of the dimeric species was pH independent, $\delta$ = 134.0 ppm, confirming that the $[Re_2O_3(CN)_4]^{4-}$ complex is unreactive toward protonation in the pH range studied.

An interesting observation in this study specifically concerned the formation of this dimeric species (Scheme I). It is known that the presence of $[ReO(OH)(CN)_4]^{2-}$ plays an important role in the formation of the $[Re_2O_3(CN)_8]^{4-}$ complex, and pH changes are expected upon formation of significant concentrations (monitored with ease by both $^{13}C$ and $^{17}O$ NMR spectroscopy) thereof. This has indeed been observed, i.e., a significant *decrease* in solution pH at pH values around 1.3 and the opposite at pH values around the $pK_{a_2}$ value (=3.72) of the aqua species, in agreement with the following equilibria:

pH ca. 1.3

$$[ReO(H_2O)(CN)_4]^- + [ReO(OH)(CN)_4]^{2-} \rightleftarrows [Re_2O_3(CN)_8]^{4-} + H^+$$

pH ca. 3.7

$$[ReO(OH)(CN)_4]^{2-} + [ReO_2(CN)_4]^{3-} + H_2O \rightleftarrows [Re_2O_3(CN)_8]^{4-} + OH^-$$

Several important conclusions can be made from the $^{17}O$ NMR study described above. Since only one signal was observed over

the entire pH range, it is concluded that, in the case of both the $[ReO(OH)(CN)_4]^{2-}$ and $[ReO(H_2O)(CN)_4]^-$ complexes, only the average signal of the enriched oxo and hydroxo/aqua sites is observed.[15] The integrals of the $^{17}O$ signals obtained at pH values of 1.8, 3.2, and 5.5, again by careful choice of repetition time as described above, were within experimental error the same, in all three cases consistent with a Re:O molar ratio of 1:2. This implies that the signal observed at pH values around 5 represents the true position of the $^{17}O$ signal of the dioxo complex ($\delta(ORe\mathit{O})$, Figure 4), both Re=*O sites being observed and equivalent. As soon as the pH is however lowered to below $pK_{a_2}$, only average signals are observed[15] (Figures 2–4).

The fact that *both* oxygen sites are enriched, hence the O:Re molar ratio of 2:1, can be explained by a rapid proton exchange according to the following scheme:[16]

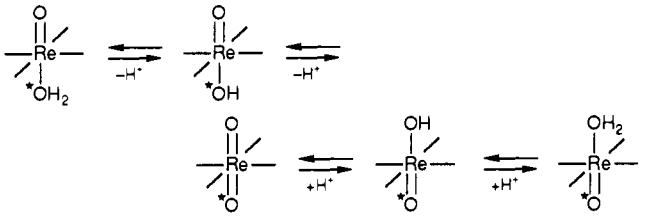

It is fair to conclude that once exchange of the $H_2O$ by a $H_2{}^*O$ from the bulk has taken place, as a result of the rapid proton exchange, the $^{17}O$ signal of the enriched metal *oxo* site is observed. It is however not the oxo ligand as such that undergoes the actual exchange with the bulk water. This is often the case in the literature where a rapid oxo exchange is reported but might be attributed to protonated forms undergoing exchange accompanied by fast proton exchange as was shown previously, in, for example, the Ti(IV) aqueous system.[17]

The values determined for the second acid dissociation constants for the $[ReO(H_2O)(CN)_4]^-$ complex in the $^{13}C$ study (Figure 1) and also from the $^{17}O$ chemical shift vs pH data (Figure 5) are in excellent agreement; see Table I. A substantial broadening (>2000 Hz) of the $^{17}O$ signal at low pH values, since it is an *average*[15] signal of the oxo/hydroxo and oxo/aqua modes, resulted in the inaccurate measurement of chemical shifts and accounts for the fact that $pK_{a_1}$ values could not be determined from $^{17}O$ chemical shift vs pH data (Figure 5). This substantial signal broadening cannot be explained at this point, but it is assumed that it is related to the proton exchange.

In the case of the $^{17}O$ solution studies described above, the chemical shift data, also those obtained in DMSO solutions, can be correlated with results from previous X-ray crystallographic and infrared solid-state studies on these oxocyanorhenate(V) complexes. An excellent comparison can be made with rhenium–oxygen bond distances as determined from crystallographic studies; see Table II. The Re—O bond strength decreases systematically from the strongest Re=O bond in $[ReO(H_2O)(CN)_4]^-$ (bond distance = 1.667 (8) Å) to the weakest Re—O bond (Re—$OH_2$ bond distance = 2.142 (7) Å) in the same aqua species. The Re=O and Re—O bonds[5] in $[ReO(OH)(CN)_4]^{2-}$, $[ReO(NCS)(CN)_4]^{2-}$, $[ReO_2(CN)_4]^{3-}$,[18] and $[Re_2O_3(CN)_8]^{4-}$ are all intermediate between these two extreme values. It is also clear that the electronic environments of the hydroxo ligand in the $[ReO(OH)(CN)_4]^{2-}$ complex and the $\mu$-O ligand in the dimeric species are quite similar, the same being true for the respective terminal oxo groups. This Re—O bond strength decrease and therefore the electron density increase on the oxygen atom correlate directly, as was found in other systems.[11,12] Furthermore, it is also of interest to note that the observed infrared stretching frequencies, $\nu$(Re—O), for all five of the Re=O bonds, as well as the Re—O bonds (in the dimeric, oxo hydroxo, and aqua oxo complexes, respectively) in the abovementioned five Re(V) complexes,[5] correlate directly with the increase in bond strength and therefore with the decrease in electron density on the oxo ligand.

This study showed that the different species in the protonation/ligation system of the $[ReO_2(CN)_4]^{3-}$ complex in solution are in direct agreement with those observed from crystallographic and infrared studies. It again demonstrated the usefulness of NMR spectroscopy, $^{13}C$, but more specifically that of $^{17}O$, in oxo systems, for characterization of species and correlation between chemical shift and the electronic environment of coordinated oxygen ligands.[19] It also demonstrated, however, that care needs to be taken before assigning observed signals to specific coordinated sites without having a knowledge of the complete system.

We are currently extending our studies to the other known $[MO_2(CN)_4]^{n-}$ systems of W(IV), Mo(IV), and Tc(V) to further investigate the effects observed in this study, concentrating on the proton- and oxygen-exchange kinetics of these and similar systems. Knowledge of the kinetic behavior of these types of model systems with regard to certain nuclear medicinal compounds is of prime importance in the development of more effective preparative techniques and the prediction of in vivo behavior of similar technetium and rhenium radiopharmaceuticals.[10,20]

**Acknowledgment.** Financial support of this research, provided by the Swiss National Science Foundation (Grant No. 20-27848.89), is gratefully acknowledged. A.R. and J.G.L. also thank the Research Fund of the University of the Orange Free State and the South African FRD for financial assistance.

(15) The average $^{17}O$ chemical shift expected for the hydroxo oxo and aqua oxo complexes in $H_2O$ can be estimated from the $^{17}O$ DMSO chemical shift data for the oxo and hydroxo/aqua signals as reported in Table II. By simple calculation, $^{17}O$ chemical shift values of 436 and 428 ppm are obtained respectively for the two complexes. This is in good agreement with the observed average chemical shift in water of 443 ppm (Table I), considering the difference in the chemical shifts of the observed $^{17}O$ signals of the $[Re^*O(NCS)(CN)_4]^{2-}$ complex in both solvents.

(16) The possible existence of a symmetrical dihydroxo species is not considered as a result of the current spectral, previously gathered X-ray structural, and more specifically kinetic evidence; see also ref 5–10.

(17) Comba, P.; Merbach, A. E. *Inorg. Chem.* **1987**, *26*, 1315.

(18) Murmann, R. K.; Schlemper, E. O. *Inorg. Chem.* **1971**, *10*, 2352.

(19) Christ, H. A.; Diehl, P.; Schneider, H. R.; Dahn, H. *Helv. Chim. Acta* **1961**, *44*, 865.

(20) Helm, L.; Deutsch, K.; Deutsch, E.; Merbach, A. E. *Helv. Chim. Acta* **1992**, *75*, 210.